PHYSICAL REVIEW A **87**, 030503(R) (2013)

# Experimental observation of the lowest levels in the photoassociation spectroscopy of the $0_g^-$ purely-long-range state of $Cs_2$

Yichi Zhang, Jie Ma,* Jizhou Wu, Lirong Wang, Liantuan Xiao, and Suotang Jia

*State Key Laboratory of Quantum Optics and Quantum Optics Devices, Laser Spectroscopy Laboratory, College of Physics and Electronic Engineering, Shanxi University, Taiyuan 030006, People's Republic of China*

(Received 16 December 2012; published 12 March 2013)

We have experimentally observed the two lowest vibrational levels of $Cs_2$ $0_g^-$ purely-long-range states. The photoassociation spectroscopy of ultracold cesium atoms with rotational structure presents clear identification of these lowest levels. Values of radiative lifetimes $\tau_{3/2} = 30.41 \pm 0.06$ ns and $\tau_{1/2} = 34.81 \pm 0.07$ ns of the $6p\,^2P_{1/2}$and $6p\,^2P_{3/2}$ atomic levels and van der Waals coefficient $C_6 = 6852 \pm 25$ a.u. of the ground-state cesium molecule are extracted, respectively.

DOI: 10.1103/PhysRevA.87.030503 PACS number(s): 33.20.−t, 37.10.Mn, 34.20.−b, 34.10.+x

Research on cold and ultracold molecules received much attention in the last decade due to important advances and potentially new applications in several domains such as quantum computing [1], few body physics, and physical chemistry [2]. The techniques that up to now have produced molecules in the ultracold temperature range mainly are magnetoassociation (MA) [3] and photoassociation (PA) [4]. PA spectroscopy of ultracold atoms has become a powerful tool for investigation of the so-called long-range molecules with classical outer turning points of several to hundreds of nanometers. In the long-range molecules, properties of the molecular states are closely related to properties of their constituent atoms. A special class of long-range molecules is called a purely-long-range (PLR) molecule. It has a classical inner turning point at a long internuclear distance where the short-range interaction due to the overlap of atomic electron clouds is negligible.

The spin-orbit coupling causes an avoided crossing between attractive and repulsive potentials correlating to different asymptotes. With increasing precision of the experiments, highly sensitive detection methods have brought significant progress in the domain of precision measurements for the PLR cesium molecule ($Cs_2$), for instance, resonant four-body interaction in cold cesium Rydberg atoms [5], absolute frequency stabilization to cesium atom molecular hyperfine transitions [6], and the $C_6$ and $a_T$ values of $Cs_2$ obtained in Ref. [7]. In these ultracold $Cs_2$ experiments, the double-well structure of the $0_g^-$ molecular state correlated to the $6S_{1/2} + 6P_{3/2}$ dissociation limit is a key feature in the process of forming ultracold molecules. The reliable description of this state is crucial, as the double-well structure of the PLR $0_g^-$ state appears as a suitable intermediate step in the course of the formation of ground-state molecules in their absolute ground state [8]. Photoassociation spectroscopy of the $Cs_2$ $0_g^-$ PLR state had been obtained by Pillet *et al.* using the ionization detection technique in 1999 [9]. Another feasible technique to directly detect the excited molecular state levels is trap-loss detection by monitoring the fluorescence yield from the trapped atoms described by Pichler *et al.* [10]. In these pioneering experiments, they obtained the "lowest" vibrational level $v' = 0$ in the $Cs_2$ $0_g^-$ state by direct observation until the vibrational series broke off. The PA spectroscopy of the PLR $0_g^-$ state of ultracold $Cs_2$ has been theoretically interpreted by Dulieu and co-workers [11,12]. They provided a precision analytical expression for the external well of the $0_g^-$ potential curve and convinced atomic lifetimes. It is very important to note that Dulieu and co-workers predicted two levels energetically below the lowest level $v' = 0$. However, experimental observation of these levels has been difficult since the overlap between the two lowest-level states and the triplet ground-state wave function is expected to be very small and it is difficult to observe the PA lines of these levels with a very low intensity [11,12]. If these two lowest levels exist, the pioneering lowest vibrational level $v' = 0$ is actually $v = 2$, and numerous experimental and theoretical studies which are based on $0_g^-$ vibrational levels, including spectroscopy and the potential curve, should be modified [6–8,13].

In this Rapid Communication, we report the experimental observation of the lowest levels of ultracold PLR cesium molecules by carrying out three-dimensional modulation PA spectroscopy. Resolved rovibrational spectra of the PLR $0_g^-(6P_{3/2})$ state are obtained. The bound energy data of the lowest levels are compared to theoretical predictions. We represent the potential curve with these data by an analytical asymptotic approach. Values of the radiative lifetimes of the $6p\,^2P_{1/2}$ and $6p\,^2P_{3/2}$ atomic levels and van der Waals coefficient $C_6$ of ground state are obtained.

The details of the experimental setup have been schematically depicted in [6]. The sample of ultracold atoms was produced in a standard vapor-loaded $^{133}$Cs magneto-optical trap (MOT) [14]. The trapping and repumping laser frequencies were locked to the Cs atomic transition $6S_{1/2}(F = 4) \rightarrow 6P_{3/2}(F' = 5)$ and $6S_{1/2}(F = 3) \rightarrow 6P_{3/2}(F' = 4)$, respectively. Figure 1(a) shows the formation and modulation scheme of photoassociative Cs molecules in the $0_g^-(6P_{3/2})$ state. The PA laser excites a pair of colliding Cs atoms into a PLR state. Ground-state ($a^3\Sigma_u^+$) molecules are formed from these excited molecules followed by spontaneous decay from the $0_g^-$ state. In PA experiments, the response time of the MOT is usually rather slow (∼1 s), thus it requires a slow scanning rate of the PA laser frequency. Therefore, a fast and effective modulation of the number of trapped cold atoms is difficult. We employ a coupling laser as an independent modulation

*Corresponding author: mj@sxu.edu.cn

 

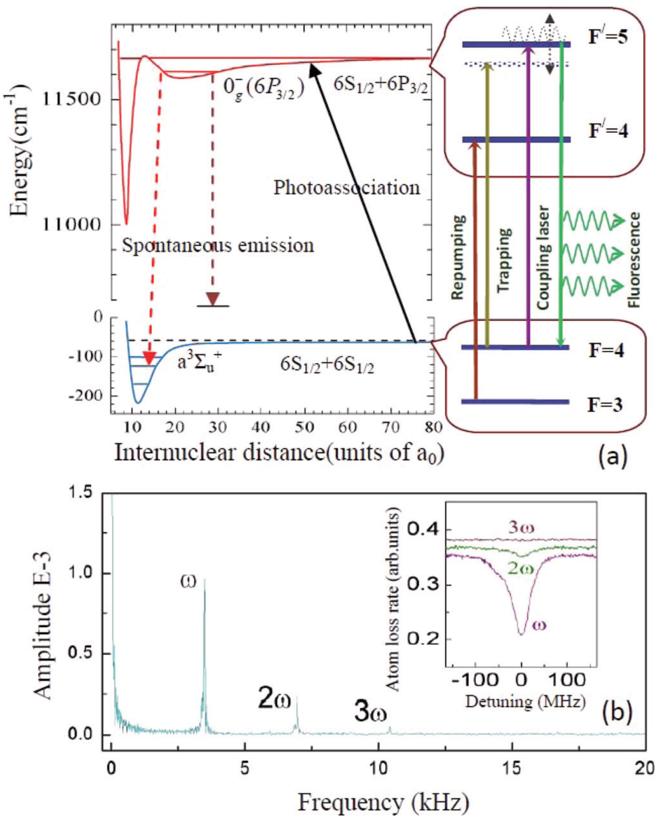


FIG. 1. (Color online) (a) Detection scheme of the improved three-dimensional fluorescence modulation spectroscopy of the $0_g^-$ state of $Cs_2$ dissociating towards the $(6S_{1/2}+6P_{3/2})$ limit. (b) Noise power spectra of cold atomic fluorescence versus modulation frequency. The inset shows the low-frequency part.

medium in order to controllably modulate the fluorescence of the trapped atoms [14,15]. The coupling laser beams, provided by a diode laser, are introduced into the center of MOT strictly along the directions of the trapping laser beams. For sine wave modulation, the instantaneous frequency of the coupling laser is $v(t) = v_0 - m\cos(2\pi\omega t)$, where $v_0$ is the carrier frequency, $m$ is the modulation index, and $\omega$ is the modulation frequency.

The intensity of the coupling laser is set to be very weak (10% of the trapping laser power), which is the best power with fewer trapped cold atoms to be heated to escape from MOT despite the maximum absorption. Note that the coupling laser frequency is the same as the trapping laser with a red detuning of $\sim$10 MHz relative to the Cs atomic resonant frequency in our measurement. We apply the optimal values of modulation index and frequency, $m = 2$ and $\omega = 3.3$ kHz. Figure 1(b) shows the noise power spectra of the cold atoms' fluorescence in MOT and the electronic noise of the detection system. The modulation signal and its high-order terms are clearly demonstrated. The demodulated signal in the first order [the purple curve in the inset of Fig. 1(b)] corresponds to a best signal-to-noise ratio (SNR) of 14.5. Therefore, we take first-order $\omega$ as the demodulation reference frequency.

Figure 2(a) describes the position of vibrational levels ($v = 2$, $v = 1$, and $v = 0$) in the $Cs_2$ $0_g^-$ external well by theory predictions [11]. In our experiment, the PA laser frequency was tuned to $\sim$11654.6 cm$^{-1}$ for observing the spectra of $v = 2$ (olive line), which was recognized as the lowest vibrational level $v' = 0$ in the previous experiments [6,9,10]. The two deeper levels are the two lowest levels $v = 1$ and $v = 0$ [purple and blue lines, shown in Fig. 2(a)], which theoretically predicted by Dulieu and co-workers are observed in our experiment. Well-resolved PA spectra of the vibrational quantum number $v = 2$ of the $0_g^-$ $(6P_{3/2})$ PLR state of $Cs_2$, whose detuning is redshifted for $\sim$77.5 cm$^{-1}$ from the $6S_{1/2} + 6P_{3/2}$ dissociation limit, is shown in Fig. 2(b). Rotationally resolved trap-loss spectra for $v = 2$ of the $Cs_2$ PLR state up to $J = 5$ is shown in the inset of Fig. 2(b). The difference (0.42 cm$^{-1}$) of rotational level energies between our spectra and the experimental spectra of Ref. [16] stems from the difference in calibration benchmark of the PA laser frequency. The line shape of the spectra for the different $J$ is the same as reported in Ref. [17]. As shown in Fig. 2(c), the PA line intensity of the vibrational level $v = 1$ of the $Cs_2$ $0_g^-$ PLR state is very small, as expected, and detuning is redshifted for $\sim$79.5 cm$^{-1}$ from the $6S_{1/2} + 6P_{3/2}$ dissociation limit. Figure 2(d) demonstrates the observed PA spectra of the lowest vibrational level $v = 0$ of the $Cs_2$ $0_g^-$ PLR state, whose detuning is redshifted for $\sim$81.6 cm$^{-1}$ from the $6S_{1/2} + 6P_{3/2}$ dissociation limit. The signal-to-noise ratio of the rotational spectra is too poor to distinguish rotational lines $J = 0$ and $J = 1$, shown in the inset of Fig. 2(d), because of the extremely tiny Franck-Condon factor. The experimental energies of the $v = 2$ and the levels of the $Cs_2$ PLR state are shown in Table I. The uncertainty is mainly due to a possible systematic error in the process of fitting and error in the determination of the resonant line position.

To represent the potential energy curve with the lowest levels of the $Cs_2$ $0_g^-$ PLR state, we have used the analytical asymptotic approach [11]. In Hund's case c representation, the $0_g^-$ $(6S_{1/2} + 6P_{3/2})$ double-well state arises from the mixing between the $^3\Pi_g(6S + 6P)$ and $^3\Sigma_g^+(6S + 6P)$ Hund's case a states. The $2 \times 2$ matrix of the Hamiltonian describing this mixing can be written as [11]

$$H = \begin{pmatrix} V^{\Pi}(R) - \Delta^{\Pi\Pi}(R) & \frac{\sqrt{2}M^2\epsilon}{9R^3} + \Delta^{\Pi\Sigma}(R) \\ \frac{\sqrt{2}M^2\epsilon}{9R^3} + \Delta^{\Pi\Sigma}(R) & V^{\Sigma}(R) \end{pmatrix}, \quad (1)$$

where the $V^{\Pi}(R)$ and $V^{\Sigma}(R)$ are the $^3\Pi_g$ and $^3\Sigma_g^+$ asymptotic potentials, $\Delta^{\Pi\Pi}(R)$ and $\Delta^{\Sigma\Pi}(R)$ are the $R$-dependent spin-orbit interactions within the $^3\Pi_g$ manifold and between the $^3\Pi_g$ and $^3\Sigma_g^+$ states, respectively. The asymptotic potentials $V^{\Pi}(R)$ and $V^{\Sigma}(R)$ are given by

$$V^{\Sigma}(R) = -\frac{C_3^{\Sigma}}{R^3}\left(1 + \frac{2\epsilon}{3}\right) - \frac{C_6^{\Sigma}}{R^6} - \frac{C_8^{\Sigma}}{R^8} + V_{\text{exch}}^{\Sigma}, \quad (2)$$

$$V^{\Pi}(R) = -\frac{C_3^{\Pi}}{R^3}\left(1 + \frac{4\epsilon}{3}\right) - \frac{C_6^{\Pi}}{R^6} - \frac{C_8^{\Pi}}{R^8} + V_{\text{exch}}^{\Pi}. \quad (3)$$

The relativistic effects are introduced in these equations as a small correction to the coefficients of the $R^{-3}$ terms [11,12], the parameter $\epsilon$ characterizing the ratio of the squared transition moments $M_{1/2}$ and $M_{3/2}$ corresponding to the relativistic $P_{1/2}$ and $P_{3/2}$ states

$$\Re = \frac{(M_{3/2})^2}{(M_{1/2})^2} = \frac{2\tau_{1/2}(\lambda_{3/2})^3}{\tau_{3/2}(\lambda_{1/2})^3} = \frac{2}{(1+\epsilon)^2}, \quad (4)$$

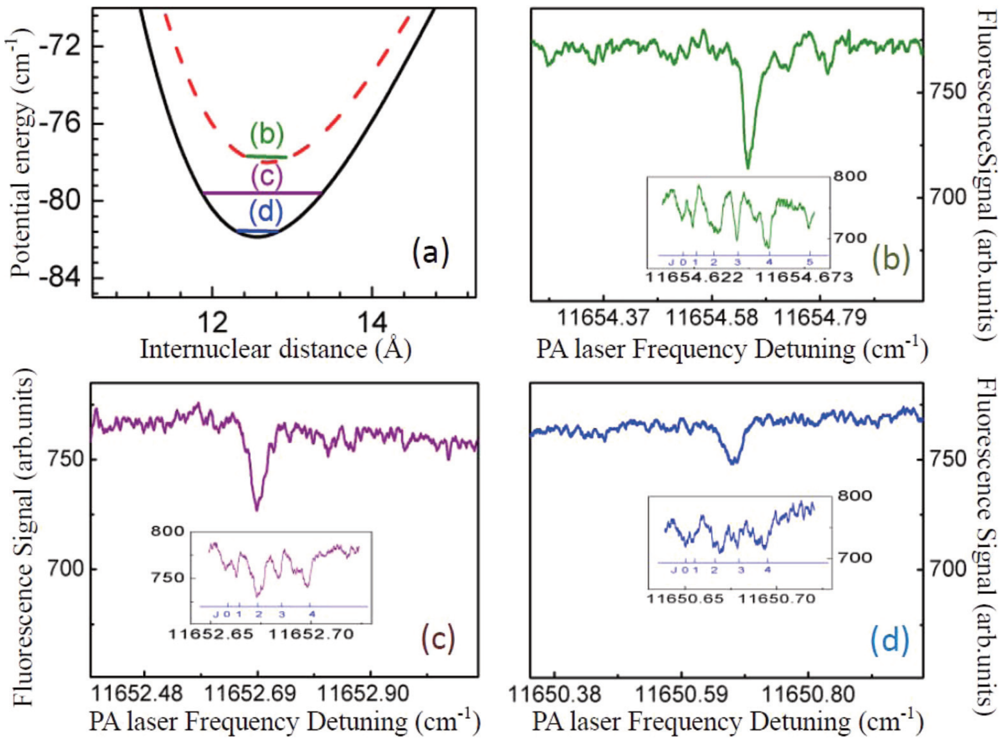


FIG. 2. (Color online) (a) Schematic of vibrational levels ($v = 2$, $v = 1$, and $v = 0$) in the potential curve of the $0_g^-$ external well are indicated by straight olive, purple, and blue lines, respectively. The vibrational spectroscopy for$v = 2$, $v = 1$, and $v = 0$ is shown in (b), (c), and (d). The insets of (b), (c), and (d) show the rotational spectroscopy for $v = 2$, $v = 1$, and $v = 0$, respectively.

where $(\lambda_{3/2})^{-1} = 11\,732.3071$ cm$^{-1}$ and $(\lambda_{1/2})^{-1} = 11\,178.2682$ cm$^{-1}$ are the $6p_{3/2,1/2} \to 6s$ transition wave numbers [12]. The $M^2$ coefficient in Eq. (1) is related to the $C_3^{\Sigma/\Pi}$ coefficients by

$$C_3^{\Pi} = -\frac{C_3^{\Sigma}}{2} = -\frac{M^2}{3}, \tag{5}$$

and it is related to the relativistic atomic transition moment corresponding to $j = 3/2$ by

$$M^2 = \frac{3}{4}(M_{3/2})^2. \tag{6}$$

The $V_{\rm exch}^{\Sigma/\Pi}$ is the exchange energy between the two atoms [18]. The spin-orbit interaction terms are given by

$$\Delta^{\Pi\Pi}(R) = \frac{\Delta E_{\rm fs}}{3}\tanh(A^{\Pi\Pi}R), \tag{7}$$

$$\Delta^{\Pi\Sigma}(R) = \frac{\sqrt{2}\Delta E_{\rm fs}}{3}\tanh(A^{\Pi\Sigma}R), \tag{8}$$

where $\Delta E_{\rm fs} = 554.039$ cm$^{-1}$ is the Cs $6p$ fine-structure splitting [11,12].

Diagonalization of the $2 \times 2$ matrix of Eq. (1) yields an analytical expression for the potential curve of the $Cs_2$ $0_g^-$ external well. We used a minimization procedure based on the so-called generalized simulated annealing (GSA) method to minimize root-mean-squared (rms) deviation [19]. Nine parameters were at first considered, as in Ref. [11]: the squared atomic transition moment $M^2$, the relativistic parameter $\epsilon$, the multipole coefficients $C_6^{\Sigma}$, $C_6^{\Pi}$, $C_8^{\Sigma}$, $C_8^{\Pi}$, the values $A^{\Pi\Pi}$ and $A^{\Pi\Sigma}$ of the spin-orbit variation parameters, and the exchange amplitude $a_{6s}a_{6p}$.

In order to obtain the best possible fit, we restricted the experimental data to the 76 lowest vibrational levels from $v = 0$ to $v = 75$, to the rotational level $J = 2$, which corresponds to and is by far the most intense line of the observed rotational progression involving $J = 0$–$6$. The experimental energy levels lying in the $Cs_2$ $0_g^-$ external well are produced with a rms of 0.0035 cm$^{-1}$. Table II presents the asymptotic parameters obtained from this analysis, together with the result of Ref. [11] and with some theoretical values [18,20]. We determine a standard deviation on the parameters by fitting 100 sets of experimental energies, obtained after adding a random

TABLE I. The experimental energies of the $v = 2$ and levels of the $Cs_2$ $0_g^-$ PLR state.

| $v$ | $E(J=0)(cm^{-1})$ | $E(J=1)(cm^{-1})$ | $E(J=2)(cm^{-1})$ | $E(J=3)(cm^{-1})$ | $E(J=4)(cm^{-1})$ | $E(J=5)(cm^{-1})$ |
|---|---|---|---|---|---|---|
| 0 | | | 11650.6667 | 11650.6801 | 11650.6970 | |
| 1 | 11652.6574 | 11652.6615 | 11652.6707 | 11652.6833 | 11652.6993 | |
| 2 | 11654.6171 | 11654.6213 | 11654.6297 | 11654.6423 | 11654.6588 | 11654.6800 |

TABLE II. Results of the present work, together with the result of Ref. [11] and with some theoretical values. The standard deviation of the parameters is indicated in parentheses.

| Parameters | This paper | Ref. [11] | Theory |
|---|---|---|---|
| $M^2(10^5\ \mathrm{cm}^{-1}\ \mathrm{Å}^3)$ | 9.808(1) | 9.806 | 10.22 [20] |
| $C_6{}^{\Pi}(10^7\ \mathrm{cm}^{-1}\ \mathrm{Å}^6)$ | 5.78(1) | 5.869 | 5.701 [20] |
| $C_6{}^{\Sigma}(10^7\ \mathrm{cm}^{-1}\ \mathrm{Å}^6)$ | 8.798(1) | 8.778 | 8.381 [20] |
| $C_8{}^{\Pi}(10^9\ \mathrm{cm}^{-1}\ \mathrm{Å}^8)$ | 3.332(3) | 3.522 | 3.045 [20] |
| $C_8{}^{\Sigma}(10^9\ \mathrm{cm}^{-1}\ \mathrm{Å}^8)$ | 17.261(3) | 17.525 | 6.802 [20] |
| $a_{6s}a_{6p}$ | 0.04150(4) | 0.04512 | 0.05479 [18] |
| $\varepsilon\ 10^{-3}$ | 4.79(2) | 4.81 | |

distribution of the experimental error bar ($\pm 0.006\ \mathrm{cm}^{-1}$) over the measured energies. The values obtained for the parameters $A^{\Pi\Sigma}$ and $A^{\Pi\Pi}$ were rather large, so that the spin-orbit interaction was hardly varying in the $R$ range of the $0_g^-$ external well. Thus, we therefore suppressed these two parameters by giving them fixed infinite values. The adjusted values for $\epsilon$, $M_2$, $C_3$, and $C_6$ are not very different from those of Ref. [11] and are in good agreement with the theoretical predictions (with a relative difference less than 5%). The value of the parameter $\epsilon = 4.79 \times 10^{-3}$ is slightly smaller compared to the values in Ref. [11]. The difference in the value of $C_8^{\Pi}$ is closer to the value in Ref. [11], a little larger compared to the theoretical value of Ref. [20] (with a relative difference less than 9%). The value of $C_8^{\Sigma}$ is a little smaller than the one in Ref. [11] but is still more than twice as large as the theoretical values of Ref. [20]. The value obtained for the asymptotic exchange amplitude $a_{6s}a_{6p}$ is closer to the one in Ref. [11] and the theoretical value of Ref. [18]. The $Cs_2$ $0_g^-$ $(6P_{3/2})$ external well potential curve is represented with and without the two lowest levels, respectively, as shown in Fig. 3. The potential minimum with the two lowest levels (black solid lines) is obtained at $R_{\min} = 12.52(1)$ Å, which is slightly smaller than without the two lowest levels[red dashed lines $R_{\min} = 12.69(1)$ Å] and with a minimum value $E_{\min} = -81.864(3)\ \mathrm{cm}^{-1}$, which is notably deeper than the red dashed one [$E_{\min} = -78.004(5)\ \mathrm{cm}^{-1}$].

The most important result of the present work is the determination of the lifetimes $\tau_{3/2}$ and $\tau_{1/2}$ of the $6P_{3/2}$ and $6P_{1/2}$ atomic levels, respectively [11]. The atomic lifetime values can be deduced from the adjusted parameter $M^2$ by

$$\tau_{3/2} = \frac{9\hbar}{4M^2}\left(\frac{\lambda_{3/2}}{2\pi}\right)^3, \tag{9}$$

$$\tau_{1/2} = \tau_{3/2}\left(\frac{\lambda_{1/2}}{\lambda_{3/2}}\right)^3 \frac{1}{(1+\epsilon)^2}, \tag{10}$$

where $M^2$ and $\epsilon$ correspond to the fit of Table I, $\tau_{3/2} = 30.44 \pm 0.06$ ns and $\tau_{1/2} = 34.81 \pm 0.07$ ns, in agreement

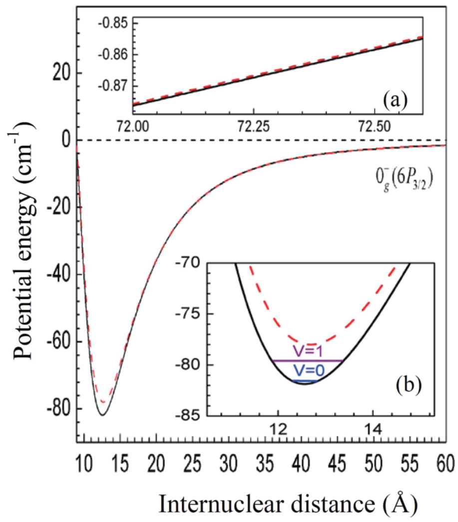


FIG. 3. (Color online) Potential curve of the PLR $0_g^-$ $(6P_{3/2})$ external well of $Cs_2$, obtained with the lowest levels $v = 1$ and $v = 0$ (black full lines) and without the lowest levels (red dashed lines). Insets (a) and (b) emphasize the differences between the two curves in the region at the large and minimum distance, respectively.

with $\tau_{3/2} = 30.41 \pm 0.30$ ns and $\tau_{1/2} = 34.82 \pm 0.36$ ns [11], $\tau_{3/2} = 30.41 \pm 0.10$ ns and $\tau_{1/2} = 34.75 \pm 0.07$ ns [21], and $\tau_{3/2} = 30.39 \pm 0.06$ ns and $\tau_{1/2} = 34.80 \pm 0.07$ ns [22]. The relative uncertainty on these values is the same as that on $M^2$ of the order of 0.2%. Moreover, we can use the method of Ref. [23] to deduce the $C_6$ coefficient by

$$C_6 = M_{1/2}^4 \xi_P + M_{1/2}^2 \xi_x + \xi_r, \tag{11}$$

where $\xi_P$, $\xi_x$, and $\xi_r$ are coefficients evaluated by [23]. From our value of $\tau_{3/2}$ and $\Re$, we can derive $M_{1/2}$ and finally obtain $C_6 = 6852 \pm 25$ a.u., in good agreement with the values $6850 \pm 140$ a.u. [11], $6860 \pm 25$ a.u. [24], and $6846 \pm 16$ a.u. [25]. The uncertainty of 0.36% in $C_6$ is estimated by considering the uncertainties on the $\xi_P$, $\xi_x$, and $\xi_r$ parameters reported in Ref. [24], and the one on $\Re$ from our analysis.

In conclusion, we report the observation of the predicted levels of PLR $Cs_2$ by PA spectroscopy, which are theoretically predicted in Ref. [11]. The vibration quantum numbers of the $Cs_2$ $0_g^-$ state are modified as $v = v' + 2$.

The authors gratefully thank Xiaomeng Liu (Shanxi University, China) and Professor Olivier Dulieu (Laboratory Aimé Cotton, France) for many valuable discussions. This research is sponsored by the 973 Program (No. 2012CB921603), the 863 Program (No. 2011AA010801), the International Science and Technology Cooperation Program of China (No. 2011DFA12490), NSF of China (No. 61008012 and No. 10934004), and RFDP (No. 2011AA010801).

[1] D. DeMille, Phys. Rev. Lett. **88**, 067901 (2002).
[2] B. Wunsch, N. T. Zinner, I. B. Mekhov, S. J. Huang, D. W. Wang, and E. Demler, Phys. Rev. Lett. **107**, 073201 (2011).
[3] O. Dulieu and C. Gabbanini, Rep. Prog. Phys. **72**, 086401 (2009).
[4] K. M. Jones, E. Tiesinga, P. D. Lett, and P. S. Julienne, Rev. Mod. Phys. **78**, 483 (2006).

[5] J. H. Gurian, P. Cheinet, P. Huillery, A. Fioretti, J. Zhao, P. L. Gould, D. Comparat, and P. Pillet, Phys. Rev. Lett. **108**, 023005 (2012).

[6] J. Ma, L. R. Wang, Y. T. Zhao, L. T. Xiao, and S. T. Jia, Appl. Phys. Lett. **91**, 161101 (2007).

[7] C. Drag, B. Laburthe Tolra, B. T'Jampens, D. Comparat, M. Allegrini, A. Crubellier, and P. Pillet, Phys. Rev. Lett. **85**, 1408 (2000).

[8] I. Manai, R. Horchani, H. Lignier, P. Pillet, D. Comparat, A. Fioretti, and M. Allegrini, Phys. Rev. Lett. **109**, 183001 (2012).

[9] A. Fioretti, D. Comparat, C. Drag, C. Amiot, O. Dulieu, F. Masnou-Seeuws, and P. Pillet, Eur. Phys. J. D **5**, 389 (1999).

[10] M. Pichler, H. M. Chen, and W. C. Stwalley, J. Chem. Phys. **121**, 6779 (2004).

[11] N. Bouloufa, A. Crubellier, and O. Dulieu, Phys. Rev. A **75**, 052501 (2007).

[12] C. Amiot, O. Dulieu, R. F. Gutterres, and F. Masnou-Seeuws, Phys. Rev. A **66**, 052506 (2002).

[13] L. Pruvost and H. Jelassi, J. Phys. B **43**, 125301 (2010).

[14] J. Z. Wu, J. Ma, Y. C. Zhang, Y. Q. Li, L. R. Wang, Y. T. Zhao, G. Chen, L. T. Xiao, and S. T. Jia, Phys. Chem. Chem. Phys. **13**, 18921 (2011).

[15] J. Z. Wu, Z. H. Ji, Y. C. Zhang, L. R. Wang, Y. T. Zhao, J. Ma, L. T. Xiao, and S. T. Jia, Opt. Lett. **36**, 2038 (2011).

[16] F. P. D. Santos, F. Perales, J. Leonard, A. Sinatra, J. M. Wang, F. S. Pavone, E. Rasel, C. S. Unnikrishnan, and M. Leduc, Eur. Phys. J. D **14**, 15 (2001).

[17] J. Ma, J. Z. Wu, Y. T. Zhao, L. T. Xiao and S. T. Jia, Opt. Express **18**, 17089 (2010).

[18] M. Marinescu and A. Dalgarno, Z. Phys. D **36**, 239 (1996).

[19] R. F. Gutteres, M. Argollo de Menezes, C. E. Fellows, and O. Dulieu, Chem. Phys. Lett. **300**, 131 (1999).

[20] M. Marinescu and A. Dalgarno, Phys. Rev. A **52**, 311 (1995).

[21] L. Young, W. T. Hill, III, S. J. Sibener, S. D. Price, C. E. Tanner, C. E. Wieman, and S. R. Leone, Phys. Rev. A **50**, 2174 (1994).

[22] A. Derevianko, J. F. Babb, and A. Dalgarno, Phys. Rev. A **63**, 052704 (2001).

[23] A. Derevianko and S. G. Porsev, Phys. Rev. A **65**, 053403 (2002).

[24] C. Chin, V. Vuletic, A. J. Kerman, S. Chu, E. Tiesinga, P. J. Leo, and C. J. Williams, Phys. Rev. A **70**, 032701 (2004).

[25] N. Vanhaecke, C. Lisdat, B. T'Jampens, D. Comparat, A. Crubellier, and P. Pillet, Eur. Phys. J. D **28**, 351 (2004).